Self-Defensive Layer-by-Layer Films with Bacteria-Triggered Antibiotic Release

Iryna Zhuk,[†] Freneil Jariwala,[†] Athula B. Attygalle,[†] Yong Wu,[‡] Matthew R. Libera,[‡] and Svetlana A. Sukhishvili[†,*]

[†]Department of Chemistry, Chemical Biology, and Biomedical Engineering, Stevens Institute of Technology, Hoboken, New Jersey 07030, United States and [‡]Department of Chemical Engineering and Materials Science, Stevens Institute of Technology, Hoboken, New Jersey 07030, United States,

ABSTRACT We report on highly efficient, bioresponsive, controlled-release antibacterial coatings constructed by direct assembly of tannic acid (TA) with one of several cationic antibiotics (tobromycin, gentamicin, and polymyxin B) using the layer-by-layer (LbL) technique. These films exhibit a distinct "self-defense" behavior triggered by acidification of the immediate environment by pathogenic bacteria, such as *Staphylococcus epidermidis* (*S. epidermidis*) or *Escherichia coli* (*E. coli*). Films assembled using spin-assisted and dip-assisted techniques show drastically different morphology, thickness and pH-/bacteria-triggered antibiotic release characteristics. While dip-deposited films have rough surfaces with island-like, granular structures regardless of the film thickness, spin-assisted LbL assemblies demonstrate a transition from linear deposition of uniform 2D films to a highly developed 3D morphology for films thicker than ~45 nm. Ellipsometry, UV—vis and mass spectrometry confirm that all coatings do not release antibiotics in phosphate buffered saline at pH 7.4 for as long as one month in the absence of bacteria and therefore do not contribute to the development of antibiotic resistance. These films do, however, release antibiotics upon pH lowering. The rate of triggered release can be controlled through the choice of assembled antibiotic and the assembly technique (spin- *vs* dip-deposition) and by the spinning rate used during deposition, which all affect the strength of TA—antibiotic binding. TA/antibiotic coatings as thin as 40 nm strongly inhibit *S. epidermidis* and *E. coli* bacterial growth both at surfaces and in surrounding medium, but support adhesion and proliferation of murine osteoblast cells. These coatings thus present a promising way to incorporate antibacterial agents at surfaces to prevent bacterial colonization of implanted biomedical devices.

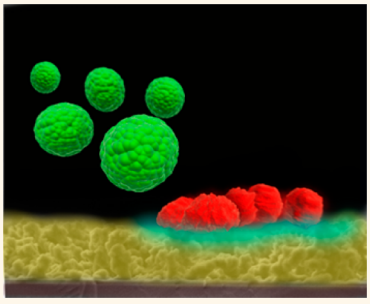

KEYWORDS: layer-by-layer films · drug release · bacteria-responsive films · antibacterial coatings · antibiotic delivery · tannic acid · pH-triggered release

Infection of biomedical devices caused by bacterial colonization of surfaces continues to remain a serious health care problem.[1,2] To thwart the development of biofilms that cause such infections, localized drug delivery aims to provide a therapeutic dose while avoiding systemic toxicity. The use of antibacterial agents to prevent infection still might be clinically unavoidable[3] despite significant progress in designing surfaces that inhibit bacterial adhesion *via* variations of surface nano- and microtopography,[4,5] creating antifouling coatings *via* surface modification with hydrophilic polymers,[6,7] or developing cationic coatings which kill on contact.[8,9]

Polyelectrolyte multilayers (PEMs) constructed using the layer-by-layer (LbL) technique[10] with their unprecedented versatility in assembly design are a unique platform to design bioactive coatings with multiple functionalities. This technique has been used to regulate bacterial adhesion,[11,12] create cationic coatings that kill on contact,[13] or include a variety of biomolecules such as proteins, enzymes, drugs and nanoparticles[14−16] without loss of their biological function within the surface coatings. Enzymatically active noneluting antibacterial LbL coatings,[17−19] films that continuously elute silver ions[20,21] or release antimicrobial compounds through biodegradation[22−24] have been previously developed. However, continuous elution of antibacterial agents presents a serious issue in the case of clinically relevant antibiotics, because of the emergence of antibiotic resistant bacteria.[25,26] Therefore, coatings that deliver therapeutic agents on demand, *i.e.*, only when and where needed, is a promising approach which also mitigates the toxicity issue and premature depletion of the drug supply/reservoir. PEM films have

* Address correspondence to ssukhish@stevens.edu.

Received for review February 3, 2014 and accepted August 5, 2014.

Published online August 05, 2014
10.1021/nn500674g

been explored as such coatings that release functional molecules in response to various environmental stimuli such as pH,[15,27,28] electric or magnetic field, ionic strength and temperature.[29−32]

pH-responsive films are a promising class of PEM film which are readily obtained by using weak polyelectrolytes in film assembly.[33−35] Importantly, the film's retention/release properties can be preprogrammed at the step of film construction by selecting the type of functional groups that serve as adsorption centers for small molecules and the assembly conditions for weak polyelectrolytes.[28,36−39] For a broad range of therapeutic molecules, incorporation and retention of small molecules within delivery films becomes an issue because of their weak binding to the films. The binding issue becomes particularly important in the case of antibiotics, whose continuous elution when not needed can contribute to the development of antibiotic resistance. Many clinically relevant antibiotics commonly used for infection treatments, such as gentamicin (Gent), tobramycin (Tob) and others, are small molecules carrying no more than 5 charges at pH 7.5. Although several successful ways of controlling elution of Gent from non-PEM[40] and PEM[23,41] degradable films have been demonstrated, the design and development of coatings able to absorb large amounts of antibiotic at physiological conditions and release these antibiotics on demand has remained illusive.

In particular, in our prior work on the sequestration and pH-triggered release of several antimicrobial compounds,[27] Gent could not be retained within an oppositely charged PEM matrix because of its low binding constant and screening of electrostrostatic interactions in physiologically relevant salt concentrations (0.15−0.2 M NaCl). Here, we overcome this challenge and report on novel and highly efficient LbL coatings obtained by the direct assembly of several antibacterial agents with tannic acid (TA), a natural tannin molecule with antitumor, antibacterial, antimutagenic, and antioxidant activities.[42] Compared to synthetic weak polyelectrolytes, such as poly(carboxylic acid)s, used earlier for constructing pH-responsive coatings, TA provides a favorable combination of electrostatic and hydrogen bonding interactions for efficient retention of antibiotics at pH 7.5 and their release at lower pH values. Unlike previously reported antibiotic-containing coatings that constantly elute antibiotics and can potentially result in the emergence of antibiotic-resistant bacteria, our films do not release antibiotics under normal, infection-free physiological conditions for as long as one month. At the same time, our films efficiently supply antibiotics locally when activated by pH lowering.

Electrostatic assembly of TA with cationic polymers was first explored by Lvov and co-workers,[43,44] while our group earlier reported on hydrogen-bonding assembly of TA with neutral polymers.[45,46] Hydrogen-bonded assembly of TA was subsequently shown to be a promising way to prepare biocompatible capsules and/or encapsulate cells.[47−49] Unlike this prior work, here TA has been assembled with low-molecular weight nonpolymeric antibiotic agents, such as Gent, Tob, and polymyxin B (PolyB), an antibiotic which can be used to prevent infections caused by multidrug-resistant pathogens.[50] Binding of all these antibiotics with TA produced films that contained large amounts of active antibiotics (~300 μg/mm^3) and were stable at pH 7.5 and physiologically relevant ionic strength.

We found that TA/antibiotic assemblies, in addition to efficient retention and on-demand release of antibiotics, showed several interesting features. When spin-assisted assembly was applied instead of the more common dipping approach, smoother films were deposited, and an unusual transition from LbL 2D film growth to irregular 3D film growth occurred. Importantly, the release rate of antibiotics was significantly slower for spin-deposited films and depended on the type of included antibiotic. We carefully examined molecular interactions and correlated differences in these interactions with the molecular structure of antibiotics used in the LbL film assembly. Using ellipsometry, UV−vis, and mass spectrometry, we quantified the pH-induced release of antibiotics from PEM films. In biological experiments involving Petrifilm antibacterial tests, films containing only 3 bilayers of TA/antibiotic with thicknesses as low as ~5 nm efficiently prevented surface colonization by Gram-positive *Staphylococcus epidermidis*. At the same time, the films were nontoxic to osteoblasts. We suggest that the antibacterial activity of TA/antibiotic coatings is triggered by the presence of *S. epidermidis* or Gram-negative *Escherichia coli*, which are known to produce acidic environments.[51,52] The concept of bacteria-triggered self-defensive delivery has been introduced in our earlier work, with the suggestion to use the acidification of the local physiological medium by bacterial colonization as a trigger,[27] but these earlier coatings did not provide useful functions under physiologically relevant conditions. The concept of self-defensive coatings has recently been explored using another triggering mechanism, *i.e.*, bacteria-induced enzymatic degradation.[53] Here, we report, for the first time, that direct LbL assembly of antibiotics with a natural polyphenol molecule results in biocompatible coatings that contain large amount of antibiotics and do not release them in infection-free physiological conditions, but demonstrate triggered antibiotic release in response to a bacterial challenge.

RESULTS AND DISCUSSION

Interactions between TA and Antibiotics in Solution. Gent, Tob and PolyB molecules carry positive charges at a physiological pH of 7.5 (Scheme 1, +4 elementary

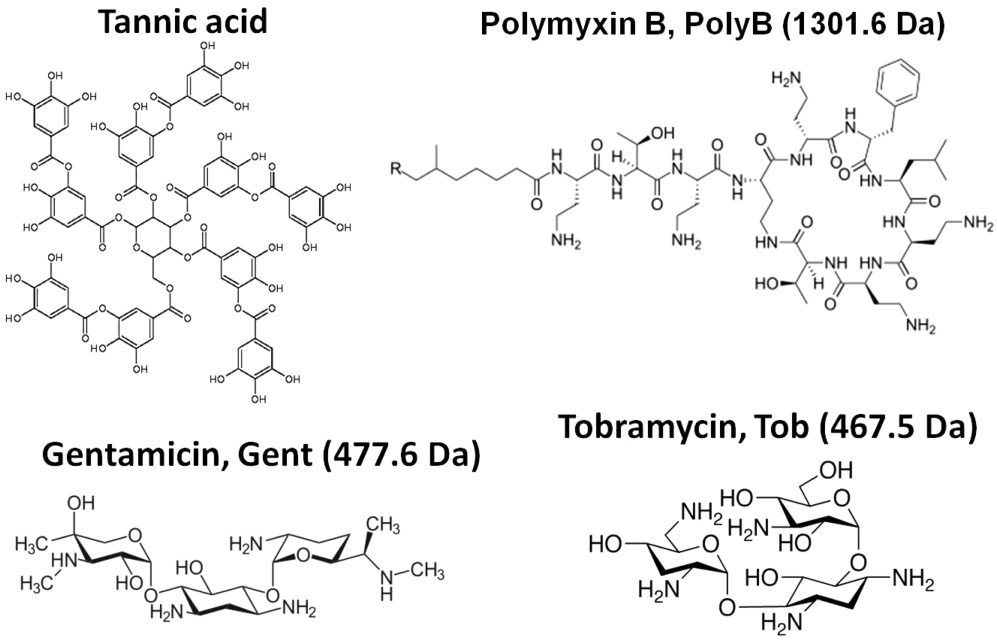

Scheme 1. Chemical structures of PEM components.

charges in Gent and +5 elementary charges in Tob and PolyB) due to protonation of primary and/or secondary amino groups. TA, a weak polyphenol acid with p$K_a \approx$ 8.5, is partially ionized at pH 7.5, and is expected to bind electrostatically with protonated amino groups of antibiotics. To probe these interactions in solution at pH 7.5, we studied the turbidity and absorbance of TA/antibiotic mixtures (Figure 1A and B, respectively). Figure 1A shows the optical density of TA/antibiotic mixtures at 420 nm, where none of the mixture components have molecular absorption bands, as a function of a molar fraction of phenol groups Φ_m [OH]. Φ_m [OH] is defined as the molar fraction of phenol groups in TA/antibiotic mixtures, *i.e.*, the ratio of the number of phenol groups in TA to the sum of the phenol groups in TA and amino groups in the antibiotic molecules.

The maximum turbidity occurred at Φ_m^{max}, which is equal to 0.80, 0.82, and 0.90 in TA/Tob, TA/Gent and TA/PolyB solutions, respectively. Assuming that the maximum turbidity developed for TA/antibiotic complexes at the point of their electric neutrality and that all primary amino groups of antibiotics were protonated, one can calculate the ionization degree of phenolic groups of TA within the TA/antibiotic complexes. These estimates give increasing values of ionization degrees of 11 $\pm$ 2, 17 $\pm$ 2 and 20 $\pm$ 2% for PolyB, Gent and Tob, respectively. This result correlates well with an increase in the density of amino groups in antibiotic molecules, from their sparse distribution in PolyB to a denser distribution in Gent and Tob. In our earlier work, we have shown that charge density in a linear cationic polymer has a critical effect on ionization of a weak polyacid;[35] here, we report a similar effect for small antibiotic molecules.

Figure 1B shows UV−vis absorption spectra of TA solutions at pH 7.5 before and after the addition of antibiotics. On the basis of the pK_a of TA $\approx$ 8.5, approximately 10% of the phenol groups are ionized at pH 7.5. Correspondingly, solutions of TA exhibited two strong bands at 225 and 290 nm, associated with neutral form of TA, and a small shoulder at a longer wavelength of 330 nm, reflecting partial ionization of TA phenol groups.[43] In mixtures of TA with antibiotics, the intensity of a 330 nm band was strongly increased at the expense of intensities at 225 and 290 nm, suggesting increased ionization of TA within TA/antibiotic complexes. These results correlate well with the turbidity data, as well as with previous reports on enhanced ionization of weak polyelectrolytes assembled with oppositely charged macromolecules within LbL films.[34,35]

Figure 1C shows that when the solution pH was changed to 4.5, maximum turbidity significantly shifted to larger Φ_m^{max} values as compared to those observed at pH 7.5 (from 0.80 to 0.92, from 0.82 to 0.95 and from 0.90 to 0.97 for TA/Tob, TA/Gent and TA/PolyB solutions, respectively). Considering that the ionization state of antibiotic molecules does not change between pH 4.5 and 7.5, these shifts reflect a decrease in TA ionization and enrichment of TA/antibiotic complexes with TA at pH 4.5. These observations provide a basis for understanding the mechanism of pH-triggered release of antibiotic molecules from LbL coatings described later in the manuscript.

Layer-by-Layer Assembly of TA with Antibiotics. We explored LbL deposition of TA/antibiotic films using both the dipping and the spin-assisted techniques. Note that the first attempt to directly incorporate Gent

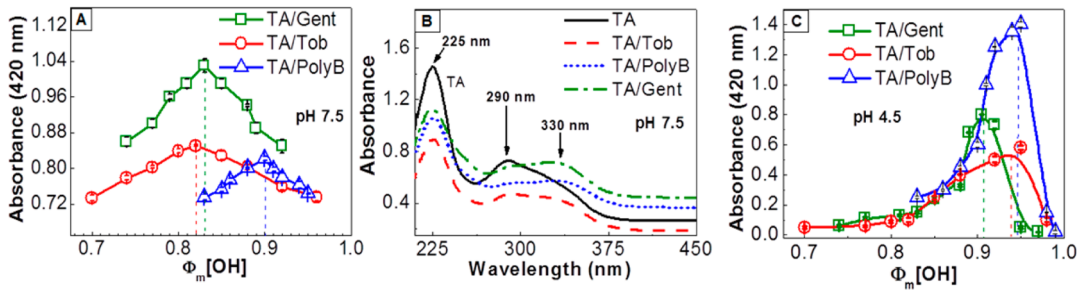

Figure 1. (A) Turbidity of TA/Gent, TA/Tob and TA/PolyB mixtures at pH 7.5 with different ratios of TA and antibiotic, obtained by mixing 2.94 μM TA and 2.09 μM antibiotic solutions at various ratios. All measurements were performed 20 min after mixing. Error bars are within a symbol size if not shown. (B) UV−vis absorption spectra of TA (black line) and TA/antibiotic complexes at Φ_m^{max} at pH 7.5. (C) Data similar to those shown in A, but for experiments performed at pH 4.5.

within a multilayer using LbL assembly was reported by Hammond and co-workers,[23] but, due to the diffusion of Gent out of the film, the stable growth of a layered structure was not achieved. Importantly, in our case, films could be successfully prepared using both deposition techniques. LbL coatings prepared by dipping had an irregular surface structure, with roughnesses as high as 12−15 nm for 3-bilayer TA/Gent films (Figure S2, Supporting Information (SI)). Figure 2 shows that the effect of spinning rate on film morphology and thickness was dramatic, with a ~4-fold decrease in surface roughness and more than a 2-fold thickness decrease for spin-assembled TA/Gent films. Additionally, as observed by many groups for the assembly of polymers within LbL films, increasingly thinner layers were deposited per each cycle because of the effects of the centrifugal force.[55,56] Previously, spin-assisted deposition has been used as a time-efficient technique to prepare LbL films with ordered internal structure using linear polymers, nanoparticles, *etc.*[55,57,58] Figure 2 illustrates that, when applied to assembly of small molecules, the spin-assisted technique has a very strong effect on film morphology, probably because of the smaller number of binding sites and therefore higher mobility of smaller molecules relative to their high-molecular-weight counterparts.

TA/antibiotic multilayer thin films could be constructed using all three types of antibiotics. Figure 3 illustrates examples of films prepared using a spinning rate of 3000 rpm. Interestingly, for all three film types a transition from linear growth of smooth 2D films to 3D (Figure S1 (SI)) films with highly developed 3D morphology occurred at ~40−45 film bilayers. At bilayer numbers smaller than 50, the film thickness increased linearly with layer number at a rate of 1.1−1.2 nm/bilayer. In contrast, the average bilayer thickness increased ~15-fold for thicker films. Note that in the 2D deposition regime, film thicknesses were readily measured by ellipsometry, but high roughness and thickness prevented us from using this technique for 3D films. Therefore, film thicknesses for films with more than 50 bilayers were estimated from scanning electron microscopy (SEM) images, and these data points are shown as stars

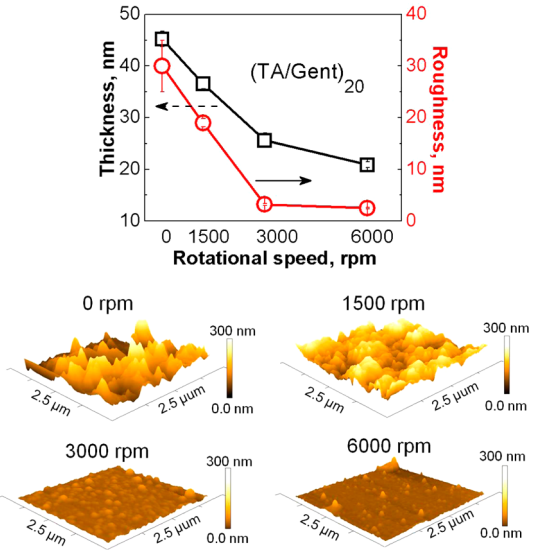

Figure 2. Effect of spinning rate on RMS roughness (determined by AFM) and ellipsometric thickness for dry $(TA/Gent)_{20}$ films deposited at pH 7.5. Shown below are representative AFM images of dip-deposited (shown as a "0 rpm" sample) and spin-assisted $(TA/Gent)_{20}$ assemblies.

in Figure 3A. From these SEM film thickness measurements together with the amounts of assembled antibiotics and TA determined by mass spectrometry and UV−vis spectrometry (see below, pH-Induced Release of Antibacterial Agents), we estimated that 3D TA/Gent films contained ~65−75% air in its dry state, *i.e.*, they present highly open, porous structures. This morphology is drastically different from that usually observed with linearly or even exponentially deposited all-polymer LbL films.[59,60]

Phenomenologically, the 2D-to-3D growth transition is reminiscent of a transition observed with films of organic molecules by molecular beam deposition,[61] but, in our case, strong molecular forces are in place, films are much less structured, and they are deposited in aqueous environments. Interestingly, the 2D−3D transition point occurs at thicknesses of 35−40 nm independent of the type of antibiotic. Figure S3 (SI) shows representative AFM images of a smooth 15-bilayer TA/Gent film (rms roughness of ~3 nm),

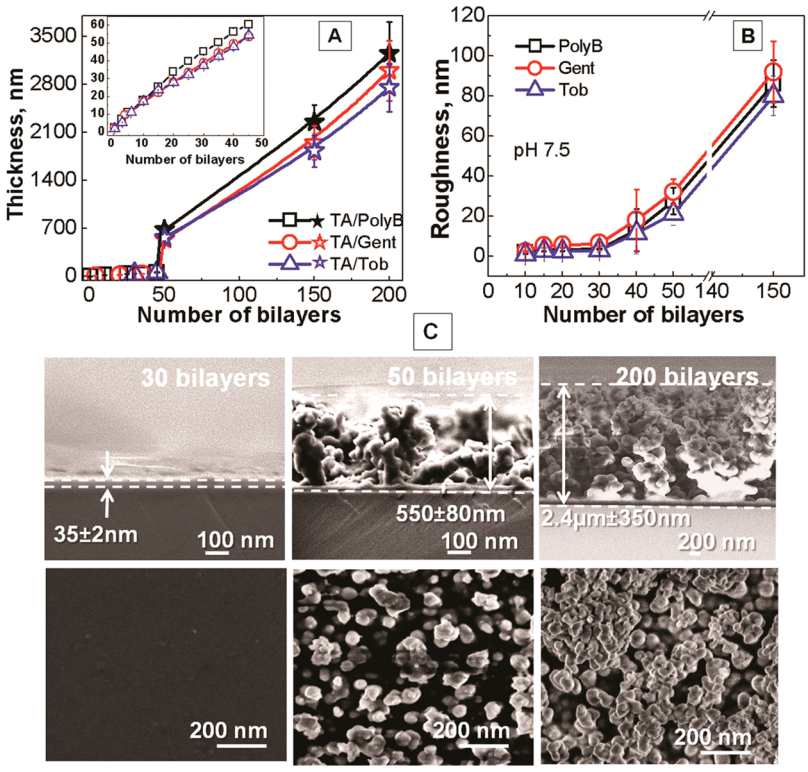

Figure 3. (A) Thickness of spin-assisted LbL deposition of TA/PolyB (squares), TA/Gent (circles) and TA/Tob (stars) films from 0.5 mg/mL TA and 0.1 mg/mL antibiotic solutions at pH 7.5 as a function of bilayer number, as monitored by ellipsometry for films with less than 50 bilayers, and by SEM for thicker films (stars). Inset shows a linear film growth regime for films with less than 45 bilayers. (B) Root-mean-square AFM roughness TA/Gent films. Error bars are within a symbol size if not shown. (C) Cross-sectional and top-view SEM images of 30-, 50- and 200-bilayer TA/Gent films.

and a drastically rougher 150-bilayer film (rms roughness of ~83 nm). Recently, the growth of similarly rough, island-like structures was reported for spray-assisted deposition of a short polyanion, poly(sodium phosphate), and a much longer polycation.[62] Unlike this prior work, our thicker films were composed of two (rather than one) distinct strata, a smooth and uniform 2D region close to the substrate and a 3D structure on top of this 2D base film (Figure 3C). For example, a $(TA/Gent)_{50}$ film was composed of a ~35 nm smooth and dense base stratum (probably reflecting the substrate-dominated growth),[63] and a rough and porous ~480 nm top layer. The double-strata deposition pattern was very consistently observed for all films with more than 40−45 bilayers. Figures 3C and S4 (SI) also show an unusual granular morphology of 3D films. The occurrence of the 2D-to-3D growth transition is probably a manifestation of the surface templating effect. Since LbL deposition and film layering is an inherently nonequilibrium phenomenon, more equilibrium-like 3D morphologies prevail in TA-antibacterial agent binding when the effect of substrate on molecular layering has sufficiently decayed. The fact that the spin-assisted deposition has a strong effect on the film morphology, and that the 2D-to-3D transition occurs at relatively small film thicknesses is probably due to the small number of binding sites between antibiotic molecules and nonlinear TA.

pH-Induced Release of Antibacterial Agents. Below, we explore the behavior of TA/antibiotic films during long-term exposure to physiological pH (pH 7.4) and ionic strength, as well as response of these films to acidic environments. pH is a particularly relevant stimulus for antibacterial coatings, since many bacteria metabolically acidify their local environment. In particular, *S. epidermidis* and *E. coli* produce lactic[51] and acetic acid,[52] respectively.

With $(TA/Gent)_{40}$ films as an example, Figure 4A shows that in solutions at pH 7.5 with 0.2 M NaCl, there were no changes in film ellipsometric thickness and no antibiotic release for as long as 35 days. One can expect consequently that, when exposed to physiological environments under normal pH and salt conditions, these films will behave as noneluting "dormant" films and not unnecessarily release antibiotic. Such unnecessary release puts pressure on bacteria to develop antibiotic resistance. At pH < 7.5, films lost a fraction of their thickness, with higher fractional losses in more acidic environments. Importantly, the release was not continuous, but the released fraction equilibrated after 1 day (Figure 4B), showing no changes at longer times. Results for other antibiotics, Tob and PolyB, were similar and are shown in Figure 4C and Figure S6 (SI). All film types were stable under physiological conditions for more than one month but lost 33−35% of

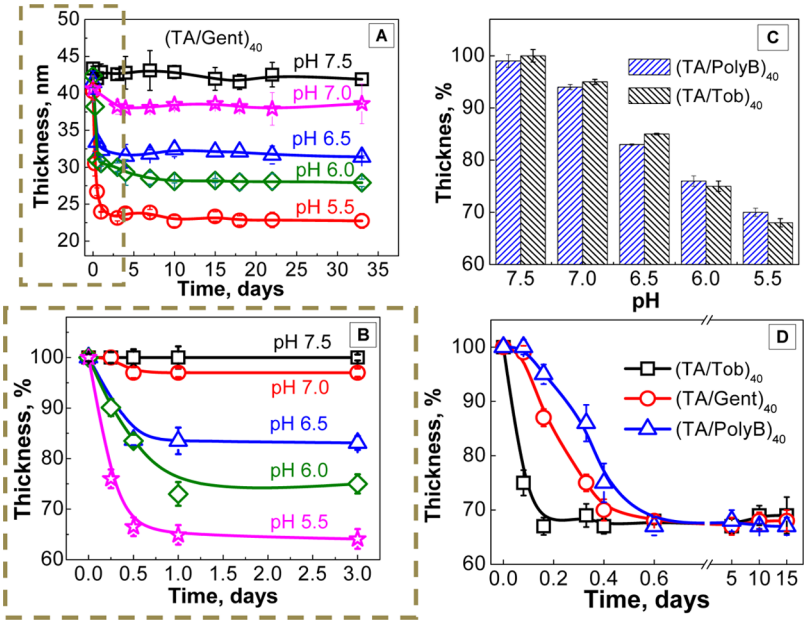

Figure 4. (A) Ellipsometry data on long-term pH-triggered release from $(TA/Gent)_{40}$ film, deposited at pH 7.5 and immersed in 0.01 M phosphate buffer solution containing 0.2 M NaCl at the range of pH 7.5 to 5.5. (B) Same data plotted on a shorter time scale. (C) Ellipsometry data on long-term pH-triggered release from $(TA/PolyB)_{40}$ (blue) and $(TA/Tob)_{40}$ (black) films, deposited at pH 7.5 and immersed in 0.01 M phosphate buffer solution containing 0.2 M NaCl at the range of pH 7.5 to 5.5. (D) Time evolution of normalized ellipsometric thicknesses of TA/Gent, TA/Tob and TA/PolyB films deposited at pH 7.5 and immersed to pH 5.5. Error bars are within symbol size if not shown.

their thickness when exposed to solutions at pH 5.5, with no changes in film thickness during long-term exposure at a constant pH. Such a release is caused by a change in charge balance within TA/antibiotic complex, when TA becomes less ionized at acidic pH. A pH-induced decrease in TA ionization leads to an accumulation of positive amino groups within the film and thus to an imbalance between negative and positive charges. In order to maintain electroneutrality at a lower pH value, TA/antibiotic films release antibiotic molecules. After this initial burst release the film becomes charge balanced; the smaller number of antibiotic molecules compensates the charge of now less-ionized TA molecules. The film thus remains stable in the environment of a lower but constant pH. Such partial, pH-triggered burst release minimizes the chance for the development of antibiotic-resistant bacterial strains, because the antibiotic remains bound within the film until some subsequent trigger releases it. Also important, pH-triggered release of a certain dose of released antibiotics is strictly determined by the degree of pH lowering, and the dose increases as the surrounding medium becomes more acidic due to metabolically active bacteria.

We also found that the short-term (<12 h) release rate depends on the type of included antibiotic. Figure 4D shows ellipsometry data for 40-bilayer TA/antibiotic films assembled at pH 7.5 and subsequently exposed to pH 5.5. Release from TA/Tob films was the fastest, while TA/PolyB films was the slowest with an initial incubation period of 6 h during which release was extremely slow. The percentage of material released from TA/Tob, TA/Gent and TA/PolyB films in 6 h was 33, 13 and 5%, respectively. At the same time, the equilibrated amounts released were similar for films with all three antibiotics. We explored the possibility that differences in the short term release kinetics in TA/antibiotic films might be attributed to various hydrophobic/hydrophilic properties of the antibiotics. The hydrophilicity of each antibiotic was estimated using the octanol:water partition coefficient (log P). Values of log *P* calculated by XLOGP2, and XLOGP3 methods provided by ALOGPS 2.1 of Advanced Chemical Development, Inc.,[64] were -2.4 ± 0.2 for PolyB, -3.6 ± 0.7 for Gent, and -6.23 ± 0.01 for Tob. These results suggest that, among these antibiotics, PolyB is the least hydrophilic, and Tob is the most hydrophilic. Hydrophilicity of bioactive molecules is known to affect the rate of their release, and an additional slower release stage has been observed with more hydrophobic drugs.[65] We suggest that with a less hydrophilic and also larger molecule among the three antibiotics, PolyB, restructuring of the LbL film required for such release is more sluggish than for films with smaller and more hydrophilic molecules. Our results corroborate these earlier observations.

In addition to its dependence on pH and on the type of antibiotic, release was also significantly affected by the technique and conditions used in film assembly. Figure 5 shows that films prepared using a spin-assisted technique were more stable, showing both a slower and smaller decrease in film thickness.

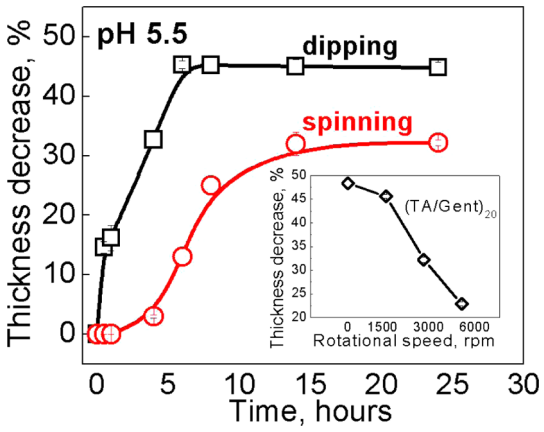

Figure 5. Ellipsometric thickness decrease for $(TA/Gent)_{20}$ films deposited at pH 7.5 by the dipping or spinning technique at 3000 rpm and exposed to pH 5.5. Inset shows the effect of the rotational speed on the equilibrated film thickness at long release times. The data point for zero rotational speed corresponds to TA/Gent films assembled by dipping.

Interestingly, spin-assisted $(TA/Gent)_{20}$ films showed a time-delayed release, which is probably due to their more ordered structure and smoother surface relative to their dip-deposited counterparts (Figure 1). While in poorly structured dip-deposited films a large surface area is readily available for immediate release of active components from the film after pH lowering, more ordered films require longer time for intermixing/rearrangements of film components in order to expose them to the film/buffer interface. Moreover, an equilibrated fraction of released material decreased ~2-fold between low (<1500 rpm) and high (6000 rpm) rotational speeds used in spin-assisted deposition. Such a strong effect of the deposition technique on the drug-release properties of TA/antibiotic films are likely a combined effect of the nonlinear nature of TA and a small number of binding sites attaching it to an antibiotic molecule, features that make these film easily prone to external fields. The fact that the deposition technique has affected both the release kinetics and the amount of released gentamicin indicates that centrifugal forces can significantly affect arrangements of intermolecular binding, and possibly stoichiometry and cooperativity of interactions of TA with antibiotics.

Since ellipsometry measurements are not specific to the chemistry of released molecules, we sought to directly quantify chemical constituents released from TA/antibiotic films. Taking the TA/Gent system as an example, we used mass spectrometry to quantify released Gent, and UV−vis spectroscopy, to evaluate the presence, if any, of TA in the film extract solution. For the mass spectrometry measurements, a set of 1 cm × 1 cm Si wafers coated at pH 7.5 with 300-bilayer TA/Gent films were exposed to a small volume (0.5 mL) of 10^{-3} M phosphate buffer containing 0.2 M NaCl at various pH values ranging from 7.5 to 5.5. In order to achieve equilibrated Gent release, we used an exposure time of 48 h. Each extract solution was then tested, and Gent was assessed using the calibration curve shown in Figure S5 (SI). Figure 6A shows the dosage of Gent released from $(TA/Gent)_{300}$ films plotted *versus* pH value in the extract solution. In agreement with the ellipsometry data above, no Gent was released at pH 7.5, and the concentration of Gent released in solution increased from 0 to 27% as the pH of the extract solution decreased from 7.5 to 5.5. Note a similar trend in a fractional decrease, but for a total film mass rather than Gent, is shown in Figure 4, where a decrease in the total film thickness at pH 5.5 was ≈33%.

The released fraction of Gent (Figure 6A, right axis) was calculated based on the total amount of antibiotic contained within the film. To determine the total content of Gent within the multilayers, $(TA/Gent)_{300}$ films were completely destroyed by exposure to an extremely acidic environment (pH 2.0), where electrostatic interactions between Gent and TA were removed because of protonation of TA, and the entire film dissolved. Mass spectrometry determined the total amount of Gent in the resulting solution to be 35 μg. Taken together with ellipsometry measurements and assuming the density of TA/Gent films to be 1 mg/cm^3, mass spectrometry measurements also determined that as-deposited at pH 7.5 TA/Gent films contained ~30% of Gent by mass or by film thickness. This corresponds to a high drug density in the film of 300 μg/mm^3, higher than 220 μg/mm^3 so far reported.[22,23,66] Figure 6B shows that during the release, the highly developed 3D structure of TA/Gent collapsed to a smoother and denser film (≈50 nm in thickness). The ~5-fold decrease in the film thickness is not directly correlated with the fraction of Gent released, but it also reflects the densification of 3D TA/Gent films which contain 70% of air in their dry state.

Finally, we addressed the question of whether Gent releases from TA/Gent films as an individual molecule, or within a complex with TA. To answer this question, we analyzed $(TA/Gent)_{50}$ film extracts for the presence of TA using UV−vis spectroscopy. Figure S7 (SI) shows that no TA emerges in solution at pH 7.5. Quantitation of TA absorbances in extract solutions at pH 5.5, together with the data in Figures 4 and 6, shows that Gent releases from the film partially as a complex with TA, and at pH 5.5 the mass ratio of released Gent and TA is 55:45. Since Gent is completely ionized at pH 5.5, and TA is weakly ionized, based on its pK_a of 8.5, the TA/Gent complex is likely to be stabilized by positive charges of Gent.

Antibacterial Activity of TA/Gent Multilayers. Gent and Tob are known to inhibit bacterial protein synthesis by irreversible binding to the 30S ribosomal subunit, while PolyB disrupts the outer membrane of bacteria by competitively displacing Ca^{2+} or Mg^{2+} ions. Gent, Tob and PolyB are used to treat both Gram-positive (*e.g.*, *S. epidermidis*) and Gram-negative (*e.g.*, *E. coli*; *Pseudomonas aeruginosa*) infections.

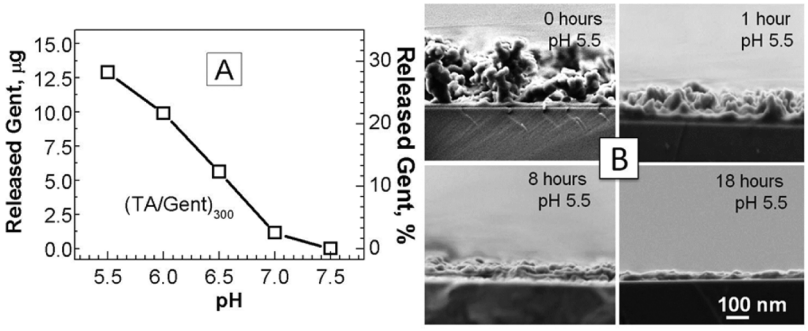

Figure 6. (A) The amount of Gent released from $(TA/Gent)_{300}$ films into 0.01 M phosphate buffer solutions containing 0.2 M NaCl at lowered pH values after 48 h, determined by mass spectrometry. Error bars are within symbol size if not shown. (B). Cross-sectional SEM images of a $(TA/Gent)_{300}$ film at different release times, indicating gradual collapse of an open 3D TA/Gent morphology during release.

The antimicrobial activity of TA/antibiotic coatings was tested with Gram-positive *S. epidermidis* ATCC 12228 and *E. coli*. (NEB #C2987; *E. coli*). To explore a possible dependence of antibacterial activity of TA/antibiotic films on the number of assembled layers, we tested 3-, 5-, 7 and 15-bilayer TA/Gent films using Petrifilm Aerobic Count Plates. A Si wafer coated with a monolayer of TA was used as a control. Figure 7A summarizes the bacterial surface coverage data, and Figure 7B shows Petrifilm images after incubation of TA/Gent LbL films with various numbers of bilayers with 10^6 bacteria/mL *S. epidermidis* for 48 h, followed by removal of Si wafers from the Petrifilm plates.

Significantly, all films (even for the thinnest ~4.5 nm 3-bilayer film) showed very efficient inhibition of bacterial colonization, with almost complete (~10^3-fold) decrease in bacterial counts. Note that TA/Gent-coated Si wafers removed from the Petrifilm plates prior to colony counting were completely free of bacterial colonization. On the basis of the mass spectrometry data (Figure 6), we have estimated the amount of eluted Gent from 3-, 5-, 7- and 15-bilayer films as 0.045 μg, 0.07 μg, 0.125 μg and 0.2 μg, respectively. Because of the small volume of buffer used in Petrifilm tests (20 μL used here), concentrations of eluted Gent were 0.9, 1.4, 2.5, and 4.1 μg/mL for 3-, 5-, 7- and 15-bilayer films, respectively—all exceeded or were within the range of the reported minimum inhibitory concentration (MIC) of Gent against *S. epidermidis* 0.06 to 4 μg/mL.[67] These results confirm that efficient release of an antibacterial agent was triggered by bacterial growth causing a pH decrease in the vicinity of TA/Gent films, and that high antibacterial efficiency of TA/Gent films can be attributed to locally high concentrations of Gent released in small volumes of liquid. Note that release from these coatings into a small-volume space is relevant for implant-associated infections, where typically a small volume of physiological liquid surrounds the implant surface.

Moreover, we studied the capacity of TA/antibiotic films to retain their activity when the films were kept in solutions at pH 7.5 for long periods of time. A set of $(TA/Gent)_{15}$ films was immersed in phosphate buffer solution with 0.2 M NaCl at pH 7.5 for as long as 4 weeks, and solutions were refreshed every 2 days. Samples were tested for antibacterial activity every week and discarded after testing. Importantly, even coatings kept at pH 7.5 for as long as 4 weeks preserved their antibacterial activity, eliminating 97% of *S. epidermidis* colonization (inset in Figure 7A). The long-term stability of these coatings is an important feature that allows use of these films as "dormant" self-defensive delivery coatings, which preserves their function for long periods of time.

To further compare the antimicrobial activity of the coatings in solution and at the surface, samples were placed in 12-well culture plates filled with 2 mL of bacterial suspension (1×10^6 colony forming units (CFU)/mL). The antimicrobial activity of $(TA/PolyB)_{15}$ coatings was tested with Gram-negative *E. coli*, and the antimicrobial activity of $(TA/Gent)_{15}$ coatings was tested with Gram-positive *S. epidermidis*. Bacterial suspension in contact with bare silicon wafers was used as a control. Figure 8A summarizes the optical density of the bacterial suspension after several hours of cell culture, and Figure 8C shows confocal laser scanning microscopy images of surface bacterial colonization. After 6, 12, and 24 h, bacterial growth in solution was significantly reduced when bacteria were cultured in the presence of $(TA/PolyB)_{15}$ and $(TA/Gent)_{15}$ films rather than with control bare silicon wafers (Figures 8A and B). This confirms that a pH decrease associated with bacterial growth (pH 6.5—5.5 measured in solution after 6—24 h), and the resulting antibiotic release from TA/antibiotic films was able to kill bacteria not only at the surface but also in the relatively large (2 mL) volumes of medium. On the basis of ellipsometry and mass spectrometry data in Figures 4 and 6, the concentration of released antibiotics in 2 mL of solution was estimated as 0.3 and 0.7 μg/mL for 6 and 24 h of bacterial culture, respectively. Both values are within the range of MIC reported for Gent against *S. epidermidis*[67] and for PolyB against *E. coli* of 0.5 μg/mL.[68] Importantly, in well plate experiments, inhibition of the surface colonization

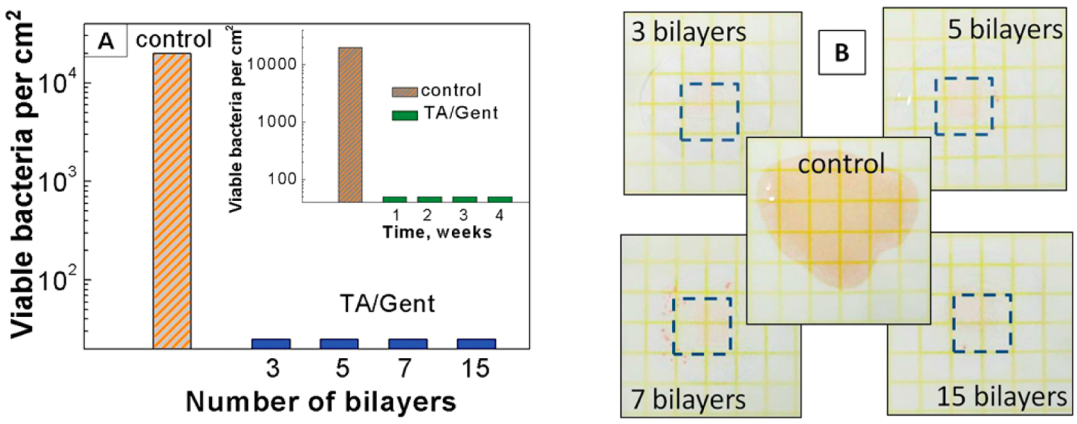

Figure 7. (A) Number of viable *S. epidermidis* bacteria per unit surface area of TA/Gent coatings with various numbers of bilayers (blue) as compared to a control Si wafer covered with a monolayer of TA (brown). Inset shows long-term antibacterial activity of $(TA/Gent)_{15}$ film exposed to *S. epidermidis* for 4 weeks (green). (B) Representative images of Petrifilm plates after incubation of 10^6 bacteria/mL *S. epidermidis* in contact with TA/Gent films for 48 h at 37 °C, followed by removal of TA/Gent-coated wafers. Error bars are within symbol size if not shown.

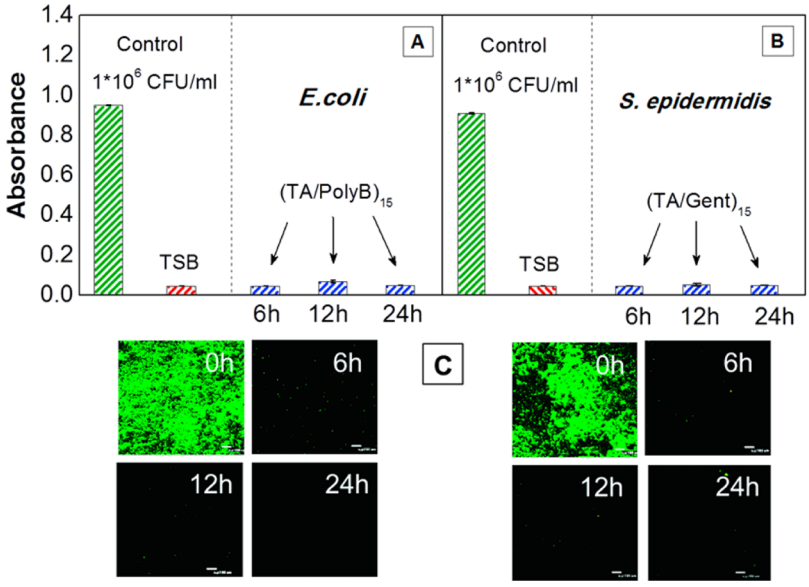

Figure 8. Growth of *E. coli* (A) and *S. epidermidis* (B) in solution in the presence of control silicon wafers after incubation for 24 h, shown together with the absorbance of TSB buffer in left subpanels, as well as in the presence of $(TA/Gent)_{15}$- and $(TA/PolyB)_{15}$-coated wafers after different incubation times in 2 mL of 1×10^6 CFU/mL bacterial suspension at 37 °C (right subpanels). (C) Confocal laser scanning microscopy images of the $(TA/Gent)_{15}$ and $(TA/PolyB)_{15}$ surfaces (left and right, respectively) after different incubation times in 2 mL of 1×10^6 CFU/mL bacterial suspension at 37 °C. The scale bar is 100 nm.

of *S. epidermidis* onto coated $(TA/Gent)_{15}$ films (Figure 8C) is consistent with our finding in Petrifilm experiments (Figure 7). Also in agreement with Petrifilm experiments, no inhibition of bacterial growth occurred on control Si wafers covered with a monolayer of TA but with no antibiotics. This conclusion is corroborated by the confocal and SEM images shown in Figure S8 (SI).

Cytocompatibility of TA/Gent Coatings. Gent has been demonstrated to be nontoxic to human osteoblasts and endothelial cells even at high dosages.[69] Here, we explore the cytocompatibility of the TA/Gent coating toward mammalian cells, *i.e.*, murine preosteoblast cells (MC3T3-E1 subclone 14 CRL-2594), which are widely used in orthopedic studies as a model of human bone cells. Nontoxicity of the TA-based film was visualized through live–dead staining at the surface coated with $(TA/Gent)_{15}$ film (Figure 9A and B) as well as at surfaces of bare silicon wafers used as a control (Figure 9C and D). Murine preosteoblast cells adhered to and proliferated on both the control wafers and wafers coated with TA/antibiotic films. Importantly, representative live/dead images indicated that the number of live cells (green) was overwhelmingly higher in comparison with the number of dead cells (red) after 1 to 4 days of culturing (Figure 9A and B), illustrating cytocompatibility of the TA/Gent coatings.

Moreover, the evolution of cell morphology differed for coated and noncoated samples. Figure 9A

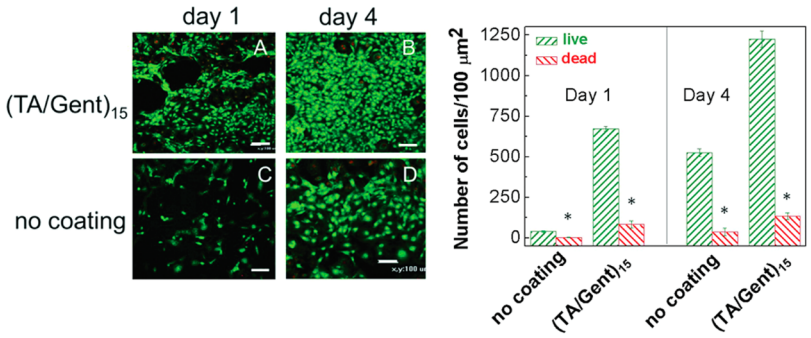

Figure 9. Confocal laser microscopy images (left) and cell viability numbers obtained by image analysis of murine preosteoblast cell attachment (right) on the surface of silicon wafers coated with $(TA/Gent)_{15}$ film (A, B) as well as on the surface of bare silicon wafers (C, D). The scale bar in (A−D) is 100 μm. Stars indicate statistically significant differences between live and dead cells as determined by the Student's *t* test ($p < 0.05$).

and B shows that after as short a culture time as 1 day, cells on top of TA/Gent coatings had well-organized cellular processes and were spindle-shaped, interconnected though tight ledges, demonstrating healthy cell growth and surface attachment. However, on uncoated control surfaces, cell morphology evolved over a longer time scale between days 1 and 4 (Figure 9C and D), at day 1 showing only round or polygonal cells with weak cell−cell interactions. This indicated that TA/Gent coatings are not only nontoxic, but also advantageous for cell attachment and proliferation of mammalian cells compared to noncoated substrates.

CONCLUSIONS

The traditional approach to design drug-delivery coatings has been based on the continuous elution of bioactive compounds. Such an approach is often undesirable for the delivery of antibiotics, because the unneeded exposure of bacteria to antibiotics can lead to the development of resistant bacterial strains. Furthermore, continuous elution ultimately depletes the coating of its antibiotic rendering the coating largely ineffective. Here, we have reported on a novel type of antibiotic-containing material with high drug content (300 μg/mm^3, 30% by mass) and noneluting properties under normal physiological conditions (pH 7.5, 0.2 M NaCl). Significantly, to create these coatings we used a natural polyphenol molecule−tannic acid (TA), rather than linear polymer molecules, which earlier were shown to be incapable of strongly retaining antibiotic molecules. In contrast to LbL films based on linear polymers, TA overcomes this limitation, probably due to its ability to involve both hydrogen bonding and electrostatic interactions in its interaction with antibiotics. Being stable and nonreleasing at pH 7.5, TA/antibiotic coatings can deliver different antibiotic doses depending on the magnitude of pH decrease. The pH signal that triggers an antibiotic burst release from TA/antibiotic coatings is created by typical bacterial pathogens, such as *S. epidermidis*, *Staphylococcus aureus* and *E. coli*, which are known to cause infections associated with many implantable biomedical devices.

We showed that the use of TA in LbL assembly results in successful inclusion of several positively charged antibiotics within these bacteria-responsive films. Examination of interactions between TA and antibiotics in solution as well as of their release from the coatings reveals the molecular mechanisms underlying the coating function, and balancing charge within the film is the driving force for dosed antibiotic release. We conclude that the strength of the molecular interactions, which are partially determined by the degree of antibiotic hydrophilicity, defines the release rate, while the degree of pH lowering correlates with the total fraction released. With these new delivery materials, we also explored the role of processing conditions on film assembly and release properties, and we report, for the first time, that not only the thickness of individual layers but also the total fraction of released drug can be controlled by the rotational speed used during spin-assisted assembly. We furthermore demonstrated that these films combine their strong antibacterial properties with noncytotoxicity toward preosteoblasts cells. These findings have far-reaching implications not only in designing smart self-defensive films that release antibiotics in response to bacterial infections but also in a broader area of assembled materials and thin films. Moreover, combining several antibiotics active against different bacteria types (*e.g.*, Gram-positive and Gram-negative) within the same film to further broaden the spectrum of antibacterial activity of these coatings might present a promising direction for future studies.

METHODS

Materials. Branched polyethylenimine (BPEI; M_w 65,000, 50% aqueous solution), tannic acid (TA; M_w 1701.20), gentamicin (Gent, 10 mg/mL aqueous solution), tobramycin (Tob), polymyxin B sulfate (PolyB), hydrochloric acid, sodium chloride, and dibasic sodium phosphate were purchased from Sigma-Aldrich

Chemical Co. Sulfuric acid was purchased from Pharmco-Aaper Co. All chemicals were used as received. *Staphylococcus epidermidis* (ATCC 35984; *S. epidermidis)* was purchased from American Type Culture Collection (ATCC). *Escherichia coli* (NEB #C2987; *E. coli*) was purchased from New England Biolabs. MC3T3-E1 subclone 14 CRL-2594 was purchased from ATCC (Manassas, VA).

D_2O with 99.9% isotope content was purchased from Cambridge Isotope Laboratories. Millipore (Milli-Q system) filtered water with a resistivity of 18.2 MΩ was used in all experiments. Silicon (110) wafers were prime grade, p/boron type, 500 ± 25 μm thick, with native oxide layer ≈2 nm, and were bought from University Wafers, Inc.

UV−Vis Measurements. UV−vis absorbance and turbidity were studied using a UV−Vis Lambda 25 spectrophotometer (PerkinElmer, Inc.). Mixing of TA with antibiotics resulted in water-insoluble complexes which were detected through increased solution scattering at 420 nm, where individual solutions of TA, Gent, Tob and PolyB have no absorption bands.

Deposition of Multilayers. TA multilayers with Gent, Tob and PolyB were deposited at the surface of Si wafers from 0.5 mg/mL TA and 0.1 mg/mL antibiotic solutions in 0.01 M phosphate buffer at pH 7.5. To remove organic impurities, silicon wafers were precleaned using a UV lamp for 2 h, treated with concentrated sulfuric acid for 20 min, rinsed with Milli-Q water and dried under flowing nitrogen. To enhance the adhesion of multilayer films to the surface, a precursor layer of BPEI was deposited at the precleaned surface from 0.5 mg/mL solution in 0.01 M phosphate buffer at pH 5.5 for 15 min. Spin-assisted LbL assembly was performed with a Laurel WS-650−23NNP/UD3/UD3B spin coater using 40-s deposition cycles and rotational rate of 1500, 3000, and 6000 rpm. The majority of experiments was performed using a rotational rate of 3000 rpm. After each deposition step, the substrates were thoroughly washed with 0.01 M phosphate buffer solution. Films were dried after the deposition of each bilayer. The speed and spinning for the rinsing step were identical to those used for film deposition.

Alternatively, LbL films were deposited using a dipping robot (DR-3, Riegler & Kirstein GmbH, Berlin) operated with custom software. Silicon wafers were alternately immersed into 0.5 mg/mL of TA and 0.1 mg/mL of antibiotic solutions at pH 7.5 for 10 min, using three intermediate rinsing steps with 0.01 M phosphate buffer.

Atomic Force Microscopy (AFM). Morphology and root-mean-square (RMS) roughness of dry films were determined in air at room temperature using an NSCRIPTOR dip pen nanolithography system (Nanoink) operating in AC tapping mode using close contact mounted cantilevers (Pacific Nanotechnology, Santa Clara, CA, USA).

Scanning Electron Microscopy (SEM). SEM images were obtained using a Zeiss Auriga Dual-Beam FIB-SEM using samples not subjected to pretreatment. Cross sectional specimens were prepared by fracturing. Silicon wafers with sample films were fixed to the SEM specimen holders with a conductive tape.

Ellipsometry. The thickness of dry thin films not exceeding 45 nm was measured using a home-built phase-modulated ellipsometer,[54] while the thickness of thicker films was determined by SEM imaging.

Mass Spectrometry. To quantify the amount of antibiotics released from TA/antibiotic films at various values of solution pH, mass spectrometric analyses were performed using an Applied Biosystems API 3000 (Concord, ON, Canada) triple quadrupole mass spectrometer equipped with a TurbolonSpray source. A Shimadzu LC-10AD (Columbia, MD, USA) HPLC system fitted with a Rheodyne 7725i (Rohnert Park, CA, USA) sample injection valve with a 20-μL loop was used for solvent delivery to the TurbolonSpray source. An isocratic solvent flow of acetonitrile−water−formic acid (50:50:0.01) was maintained at 1.0 mL/min. The source temperature was held at 550 °C. Both the nebulizer gas (N_2) and curtain gas (N_2) flow rate settings were set at 15 (arbitrary units). The drying gas (N_2) was maintained at a flow rate of 7 L/min at 60 psi. The ion spray voltage was held at 5500 V, and a declustering potential of 50 V was used. The instrument was operated in MS1 mode, and spectra were acquired from *m/z* 320 to 326 Da at 0.1 s/scan.

To quantify the amount of Gent released from a film, a calibration curve using Tob as an internal standard was developed using four calibration standards (5, 10, 20, 30 μg/mL Gent) each containing 50 μg/mL Tob (Figure S5 (SI)). The characteristic spectral peaks used for the quantitation of Gent and Tob (internal standard) were *m/z* 322 and 324, respectively, representing the protonated A and B rings (Schemes S1 and S2 (SI)). Samples from silicon wafers coated with the $(TA/Gent)_{300}$ film, which were exposed for 48 h to 0.01 M phosphate buffer solutions at pH values from 7.5 to 5.5, were evaluated. Calibration standards and Gent-containing solutions (spiked with 50 μg/mL of Tob) were directly injected into the chromatographic solvent stream, and mass spectra were continuously acquired. An average mass spectrum of 120 scans was used for each sample/standard, and mass spectral peak areas (for *m/z* 322 and 324) were integrated using Analyst 1.4.2 software.

Bacterial Strains and Growth Conditions. *S. epidermidis* or *E. coli* were incubated in tryptic soy broth (TSB) supplemented with 6 mg/mL yeast extract and 8 mg/mL glucose for 18 h. The incubated biofilm was vortexed and passed through a 5 μm filter in order to create a near single-cell suspension. The suspension was subsequently diluted to 1×10^6 CFU/mL. Before bacterial inoculation, the sample surfaces were exposed to UV light for 5 min. Samples were then incubated in 2 mL of bacterial suspension for 24 h at 37 °C in 12-well culture plates. The samples were then rinsed with phosphate buffered saline (PBS) twice before fluorescence labeling.

Quantification of *S. epidermidis* and *E. coli* Growth in Solutions. Si wafers coated with $(TA/Gent)_{15}$ and $(TA/PolyB)_{15}$ films were placed in 12-well culture plates filled with 2 mL of *S. epidermidis or E. coli* bacterial suspension (1×10^6 CFU/mL) and incubated at 37 °C for different periods of time to achieve different pH values. The optical densities of these solutions were then measured at 600 nm using a UV−vis Spectrometer Lambda 40.

Petrifilm Count Plate Procedure. All 3 M Petrifilm Aerobic Count Plates (Nelson-Jameson, Marshfield, WI, USA) were labeled and preswollen with 1 mL of sterile demineralized water for 30 min. Silicon wafers coated with $(TA/Gent)_n$ (n = 3, 5, 7, 15) films were sterilized by dipping into 70% isopropyl alcohol (IPA) for 30 min and dried. The Petrifilm cover was peeled back and the tested surfaces with the antibacterial coating facing up were placed in the center of the swollen regions. 20 μL of bacterial suspension at a concentration of 1×10^6 CFU/mL were placed on the upper edge of the surface, and the cover of the Petrifilm was carefully closed so that the bacterial suspension became uniformly distributed across the surface. The Petrifilm plates were then incubated at 37 °C for 48 h. The number of viable bacteria was determined by counting the number of colony forming units (appearing red in the Petrifilm plates) per unit area.

Osteoblast Cell Culture. Murine preosteoblast cells (MCTC3) were used to demonstrate the nontoxicity of TA/Gent films. Cells were cultured in the Dulbeccco's Modified Eagle Medium-Low Glucose (DMEM-LG; Life Technologies, NY) supplemented with antibiotic solution (1% penicillin-streptomycin; Gibco) and 10% fetal bovine serum (Atlanta Biologicals, USA). Cells were incubated in a humidified atmosphere of 5% CO_2 at 37 °C. This medium was changed daily.

Cell Seeding on LbL Films. Before their use in cell-culture experiments, silicon wafers coated with $(TA/Gent)_{15}$ films were sterilized by dipping into 70% IPA followed by washing three times in PBS at pH 7.4, and three times in fresh medium. Samples were then placed in the wells of a 6-well microtiter plate, and 50 μL of murine preosteoblast cells suspension containing 2×10^4 cells was pipetted onto each wafer. The samples were subsequently incubated in a humidified atmosphere of 4% CO_2 at 37 °C, and the medium was refreshed every day. After 1, 2, 3, and 4 days, wafers were removed from the medium and characterized for cell attachment and live/dead viability.

Live/Dead Cell Viability. Using a live/dead cell staining kit (Invitrogen), viable and nonviable cells were observed after days 1 to 4 of cell culturing. The cells were double-stained based on membrane integrity and intracellular esterase activity as per the manufacturer's protocols by incubation at room temperature for 15 min in Milli-Q solutions containing 2 μM SYTOX

nucleic acid stain (green) and 1 μM propidium iodide (red). Live (green) and dead (red) stained cells were characterized using a Zeiss LSM 5 PASCAL confocal scanning system (Carl Zeiss MicroImaging, Inc., Germany) equipped with C-Apochromat 63× 1.2 W Corr water-immersion objective lens. The number of live and dead cells per unit area in confocal images was determined using an ImageJ software. Statistical analysis was performed using the Student's *t* test.

Conflict of Interest: The authors declare no competing financial interest.

Acknowledgment. This research project has been partially supported by the Army Research Office through Grant #W911NF-12-1-0331. We are grateful to C. Agresti for her help with the cell culture preparations. The authors would also like to acknowledge A. Zhuk for his help with confocal imaging and Y. Wang for his help with the SEM imaging.

Supporting Information Available: Cross-sectional SEM images for 100 and 200 bilayers of TA/Tob and TA/PolyB films, AFM topography images for dip- and spin-assisted of TA/Gent films, top view SEM images of 30-, 50- and 200-bilayer TA/Gent films, mass spectrometric calibration curve of the concentration of Gent, ellipsometry data on long-term, pH-triggered release of tobramycin and polymyxin B from 40-bilayer TA/antibiotic films, UV−vis absorption spectra of $(TA/Gent)_{50}$ film extracts at different pH values, SEM and confocal images of bacterial colonization of TA monolayers and TA/Gent multilayers, and proposed fragmentation mechanism for the formation of the *m/z* 322 ion and *m/z* 324 ion of gentamicin and tobramycin species, respectively. This material is available free of charge *via* the Internet at http://pubs.acs.org.

REFERENCES AND NOTES

1. Campoccia, D.; Montanaro, L.; Arciola, C. R. The Significance of Infection Related to Orthopedic Devices and the Issue of Antibiotic Resistance. *Biomaterials* **2006**, *27*, 2331–2339.
2. Arciola, C. R.; Campoccia, D.; Speziale, P.; Montanaro, L.; Costerton, J. W. Biofilm Formation in Staphylococcus Implant Infections. A Review of Molecular Mechanisms and Implications for Biofilm-Resistant Materials. *Biomaterials* **2012**, *33*, 5967–5982.
3. Hetrick, E. M.; Schoenfisch, M. H. Reducing Implant-Related Infections: Active Release Strategies. *Chem. Soc. Rev.* **2006**, *35*, 780–789.
4. Fadeeva, E.; Truong, V. K.; Stiesch, M.; Chichkov, B. N.; Crawford, R. J.; Wang, J.; Ivanova, E. P. Bacterial Retention on Superhydrophobic Titanium Surfaces Fabricated by Femtosecond Laser Ablation. *Langmuir* **2011**, *27*, 3012–3019.
5. Dong, Y.; Li, X.; Bell, T.; Sammons, R.; Dong, H. Surface Microstructure and Antibacterial Property of an Active-Screen Plasma Alloyed Austenitic Stainless Steel Surface with Cu and N. *Biomed. Mater.* **2010**, *5*, 1–8.
6. Park, K. D.; Kim, Y. S.; Han, D. K.; Kim, Y. H.; Lee, E. H. B.; Suh, H.; Choi, K. S. Bacterial Adhesion on PEG Modified Polyurethane Surfaces. *Biomaterials* **1998**, *19*, 851–859.
7. Boulmedais, F.; Frisch, B.; Etienne, O.; Lavalle, P.; Picart, C.; Ogier, J.; Voegel, J. C.; Schaaf, P.; Egles, C. Polyelectrolyte Multilayer Films with Pegylated Polypeptides as a New Type of Anti-Microbial Protection for Biomaterials. *Biomaterials* **2004**, *25*, 2003–2011.
8. Gottenbos, B.; van der Mei, H. C.; Klatter, F.; Nieuwenhuis, P.; Busscher, H. J. *In Vitro* and *In Vivo* Antimicrobial Activity of Covalently Coupled Quaternary Ammonium Silane Coatings on Silicone Rubber. *Biomaterials* **2002**, *23*, 1417–1423.
9. Schaer, T. P.; Stewart, S.; Hsu, B. B.; Klibanov, A. M. Hydrophobic Polycationic Coatings that Inhibit Biofilms and Support Bone Healing during Infection. *Biomaterials* **2012**, *33*, 1245–1254.
10. Decher, G.; Hong, J. D.; Schmitt, J. Buildup of Ultrathin Multilayer Films by a Self-Assembly Process: III. Consecutively Alternating Adsorption of Anionic and Cationic Polyelectrolytes on Charged Surfaces. *Thin Solid Films* **1992**, *210−211* (Part 2), 831–835.
11. Fu, J.; Ji, J.; Yuan, W.; Shen, J. Construction of Anti-Adhesive and Antibacterial Multilayer Films *via* Layer-by-Layer Assembly of Heparin and Chitosan. *Biomaterials* **2005**, *26*, 6684–6692.
12. Lichter, J. A.; Thompson, M. T.; Delgadillo, M.; Nishikawa, T.; Rubner, M. F.; Van Vliet, K. J. Substrata Mechanical Stiffness Can Regulate Adhesion of Viable Bacteria. *Biomacromolecules* **2008**, *9*, 1571–1578.
13. Lichter, J. A.; Rubner, M. F. Polyelectrolyte Multilayers with Intrinsic Antimicrobial Functionality: The Importance of Mobile Polycations. *Langmuir* **2009**, *25*, 7686–7694.
14. Rudra, J. S.; Dave, K.; Haynie, D. T. Antimicrobial Polypeptide Multilayer Nanocoatings. *J. Biomater. Sci., Polym. Ed.* **2006**, *17*, 1301–1315.
15. Kim, B.-S.; Park, S. W.; Hammond, P. T. Hydrogen-Bonding Layer-by-Layer-Assembled Biodegradable Polymeric Micelles as Drug Delivery Vehicles from Surfaces. *ACS Nano* **2008**, *2*, 386–392.
16. Kotov, N. A.; Dekany, I.; Fendler, J. H. Layer-by-Layer Self-Assembly of Polyelectrolyte-Semiconductor Nanoparticle Composite Films. *J. Phys. Chem.* **1995**, *99*, 13065–13069.
17. Pavlukhina, S. V.; Kaplan, J. B.; Xu, L.; Chang, W.; Yu, X.; Madhyastha, S.; Yakandawala, N.; Mentbayeva, A.; Khan, B.; Sukhishvili, S. A. Noneluting Enzymatic Antibiofilm Coatings. *ACS Appl. Mater. Interfaces* **2012**, *4*, 4708–4716.
18. Nepal, D.; Balasubramanian, S.; Simonian, A. L.; Davis, V. A. Strong Antimicrobial Coatings: Single-Walled Carbon Nanotubes Armored with Biopolymers. *Nano Lett.* **2008**, *8*, 1896–1901.
19. Swartjes, J. J. T. M.; Das, T.; Sharifi, S.; Subbiahdoss, G.; Sharma, P. K.; Krom, B. P.; Busscher, H. J.; van der Mei, H. C. A Functional DNase I Coating to Prevent Adhesion of Bacteria and the Formation of Biofilm. *Adv. Funct. Mater.* **2013**, *23*, 2843–2849.
20. Agarwal, A.; Weis, T. L.; Schurr, M. J.; Faith, N. G.; Czuprynski, C. J.; McAnulty, J. F.; Murphy, C. J.; Abbott, N. L. Surfaces Modified with Nanometer-Thick Silver-Impregnated Polymeric Films that Kill Bacteria but Support Growth of Mammalian Cells. *Biomaterials* **2010**, *31*, 680–690.
21. Malcher, M.; Volodkin, D.; Heurtault, B.; André, P.; Schaaf, P.; Möhwald, H.; Voegel, J.-C.; Sokolowski, A.; Ball, V.; Boulmedais, F.; *et al.* Embedded Silver Ions-Containing Liposomes in Polyelectrolyte Multilayers: Cargos Films for Antibacterial Agents. *Langmuir* **2008**, *24*, 10209–10215.
22. Shukla, A.; Avadhany, S. N.; Fang, J. C.; Hammond, P. T. Tunable Vancomycin Releasing Surfaces for Biomedical Applications. *Small* **2010**, *6*, 2392–2404.
23. Chuang, H. F.; Smith, R. C.; Hammond, P. T. Polyelectrolyte Multilayers for Tunable Release of Antibiotics. *Biomacromolecules* **2008**, *9*, 1660–1668.
24. Shukla, A.; Fleming, K. E.; Chuang, H. F.; Chau, T. M.; Loose, C. R.; Stephanopoulos, G. N.; Hammond, P. T. Controlling the Release of Peptide Antimicrobial Agents from Surfaces. *Biomaterials* **2010**, *31*, 2348–2357.
25. Stewart, P. S.; Costerton, J. W. Antibiotic Resistance of Bacteria in Biofilms. *Lancet* **2001**, *358*, 135–138.
26. Taubes, G. The Bacteria Fight Back. *Science* **2008**, *321*, 356–361.
27. Pavlukhina, S.; Lu, Y.; Patimetha, A.; Libera, M.; Sukhishvili, S. Polymer Multilayers with pH-Triggered Release of Antibacterial Agents. *Biomacromolecules* **2010**, *11*, 3448–3456.
28. Chung, A. J.; Rubner, M. F. Methods of Loading and Releasing Low Molecular Weight Cationic Molecules in Weak Polyelectrolyte Multilayer Films. *Langmuir* **2002**, *18*, 1176–1183.
29. Kozlovskaya, V.; Kharlampieva, E.; Erel, I.; Sukhishvili, S. A. Multilayer-Derived, Ultrathin, Stimuli-Responsive Hydrogels. *Soft Matter* **2009**, *5*, 4077–4087.
30. Schmidt, D. J.; Moskowitz, J. S.; Hammond, P. T. Electrically Triggered Release of a Small Molecule Drug from a Polyelectrolyte Multilayer Coating. *Chem. Mater.* **2010**, *22*, 6416–6425.
31. Pavlukhina, S.; Sukhishvili, S. Polymer Assemblies for Controlled Delivery of Bioactive Molecules from Surfaces. *Adv. Drug Delivery Rev.* **2011**, *63*, 822–836.

32. Zhu, Z.; Gao, N.; Wang, H.; Sukhishvili, S. A. Temperature-Triggered on-Demand Drug Release Enabled by Hydrogen-Bonded Multilayers of Block Copolymer Micelles. *J. Controlled Release* **2013**, *171*, 73–80.
33. Mauser, T.; Déjugnat, C.; Sukhorukov, G. B. Reversible pH-Dependent Properties of Multilayer Microcapsules Made of Weak Polyelectrolytes. *Macromol. Rapid Commun.* **2004**, *25*, 1781–1785.
34. Shiratori, S. S.; Rubner, M. F. pH-Dependent Thickness Behavior of Sequentially Adsorbed Layers of Weak Polyelectrolytes. *Macromolecules* **2000**, *33*, 4213–4219.
35. Kharlampieva, E.; Sukhishvili, S. A. Ionization and pH Stability of Multilayers Formed by Self-Assembly of Weak Polyelectrolytes. *Langmuir* **2003**, *19*, 1235–1243.
36. Kharlampieva, E.; Sukhishvili, S. A. Release of a Dye from Hydrogen-Bonded and Electrostatically Assembled Polymer Films Triggered by Adsorption of a Polyelectrolyte. *Langmuir* **2004**, *20*, 9677–9685.
37. Tomita, S.; Sato, K.; Anzai, J.-i. Layer-by-Layer Assembled Thin Films Composed of Carboxyl-Terminated Poly(amidoamine) Dendrimer as a pH-Sensitive Nano-device. *J. Colloid Interface Sci.* **2008**, *326*, 35–40.
38. Jiang, B. B.; Li, B. Y. Tunable Drug Loading and Release from Polypeptide Multilayer Nanofilms. *Int. J. Nanomed.* **2009**, *4*, 37–53.
39. Kharlampieva, E.; Erel-Unal, I.; Sukhishvili, S. A. Amphoteric Surface Hydrogels Derived from Hydrogen-Bonded Multilayers: Reversible Loading of Dyes and Macromolecules. *Langmuir* **2006**, *23*, 175–181.
40. Price, J. S.; Tencer, A. F.; Arm, D. M.; Bohach, G. A. Controlled Release of Antibiotics from Coated Orthopedic Implants. *J. Biomed. Mater. Res.* **1996**, *30*, 281–286.
41. Moskowitz, J. S.; Blaisse, M. R.; Samuel, R. E.; Hsu, H.-P.; Harris, M. B.; Martin, S. D.; Lee, J. C.; Spector, M.; Hammond, P. T. The Effectiveness of the Controlled Release of Gentamicin from Polyelectrolyte Multilayers in the Treatment of *Staphylococcus aureus* Infection in a Rabbit Bone Model. *Biomaterials* **2010**, *31*, 6019–6030.
42. Akagawa, M.; Suyama, K. Amine Oxidase-like Activity of Polyphenols. *Eur. J. Biochem.* **2001**, *268*, 1953–1963.
43. Shutava, T.; Prouty, M.; Kommireddy, D.; Lvov, Y. pH Responsive Decomposable Layer-by-Layer Nanofilms and Capsules on the Basis of Tannic Acid. *Macromolecules* **2005**, *38*, 2850–2858.
44. Shutava, T. G.; Lvov, Y. M. Nano-engineered Microcapsules of Tannic Acid and Chitosan for Protein Encapsulation. *J. Nanosci. Nanotechnol.* **2006**, *6*, 1655–1661.
45. Erel-Unal, I.; Sukhishvili, S. A. Hydrogen-Bonded Multilayers of a Neutral Polymer and a Polyphenol. *Macromolecules* **2008**, *41*, 3962–3970.
46. Erel-Unal, I.; Sukhishvili, S. A. Hydrogen-Bonded Hybrid Multilayers: Film Architecture Controls Release of Macromolecules. *Macromolecules* **2008**, *41*, 8737–8744.
47. Kozlovskaya, V.; Kharlampieva, E.; Drachuk, I.; Cheng, D.; Tsukruk, V. V. Responsive Microcapsule Reactors Based on Hydrogen-Bonded Tannic Acid Layer-by-Layer Assemblies. *Soft Matter* **2010**, *6*, 3596–3608.
48. Chen, J.; Kozlovskaya, V.; Goins, A.; Campos-Gomez, J.; Saeed, M.; Kharlampieva, E. Biocompatible Shaped Particles from Dried Multilayer Polymer Capsules. *Biomacromolecules* **2013**, *14*, 3830–3841.
49. Kozlovskaya, V.; Zavgorodnya, O.; Chen, Y.; Ellis, K.; Tse, H. M.; Cui, W.; Thompson, J. A.; Kharlampieva, E. Ultrathin Polymeric Coatings Based on Hydrogen-Bonded Polyphenol for Protection of Pancreatic Islet Cells. *Adv. Funct. Mater.* **2012**, *22*, 3389–3398.
50. Zavascki, A. P.; Goldani, L. Z.; Li, J.; Nation, R. L. Polymyxin B for the Treatment of Multidrug-Resistant Pathogens: a Critical Review. *J. Antimicrob. Chemother.* **2007**, *60*, 1206–1215.
51. Handke, L. D.; Rogers, K. L.; Olson, M. E.; Somerville, G. A.; Jerrells, T. J.; Rupp, M. E.; Dunman, P. M.; Fey, P. D. *Staphylococcus epidermidis* saeR is an Effector of Anaerobic Growth and a Mediator of Acute Inflammation. *Infect. Immun.* **2008**, *76*, 141–152.
52. Andersen, K. B.; Von Meyenburg, K. Are Growth Rates of *Escherichia coli* in Batch Cultures Limited by Respiration? *J. Bacteriol.* **1980**, *144*, 114–123.
53. Cado, G.; Aslam, R.; Seon, L.; Garnier, T.; Fabre, R.; Parat, A.; Chassepot, A.; Voegel, J. C.; Senger, B.; Schneider, F.; *et al.* Self-Defensive Biomaterial Coating Against Bacteria and Yeasts: Polysaccharide Multilayer Film with Embedded Antimicrobial Peptide. *Adv. Funct. Mater.* **2013**, *23*, 4801–4809.
54. Pristinski, D.; Kozlovskaya, V.; Sukhishvili, S. A. Determination of Film Thickness and Refractive Index in One Measurement of Phase-Modulated Ellipsometry. *J. Opt. Soc. Am. A* **2006**, *23*, 2639–2644.
55. Chiarelli, P. A.; Johal, M. S.; Casson, J. L.; Roberts, J. B.; Robinson, J. M.; Wang, H. L. Controlled Fabrication of Polyelectrolyte Multilayer Thin Films Using Spin-Assembly. *Adv. Mater.* **2001**, *13*, 1167–1171.
56. Hall, D. B.; Underhill, P.; Torkelson, J. M. Spin Coating of Thin and Ultrathin Polymer Films. *Polym. Eng. Sci.* **1998**, *38*, 2039–2045.
57. Cho, J.; Char, K.; Hong, J. D.; Lee, K. B. Fabrication of Highly Ordered Multilayer Films using a Spin Self-Assembly Method. *Adv. Mater.* **2001**, *13*, 1076–1078.
58. Jiang, C.; Markutsya, S.; Tsukruk, V. V. Collective and Individual Plasmon Resonances in Nanoparticle Films Obtained by Spin-Assisted Layer-by-Layer Assembly. *Langmuir* **2003**, *20*, 882–890.
59. Xu, L.; Pristinski, D.; Zhuk, A.; Stoddart, C.; Ankner, J. F.; Sukhishvili, S. A. Linear *versus* Exponential Growth of Weak Polyelectrolyte Multilayers: Correlation with Polyelectrolyte Complexes. *Macromolecules* **2012**, *45*, 3892–3901.
60. Porcel, C.; Lavalle, P.; Decher, G.; Senger, B.; Voegel, J. C.; Schaaf, P. Influence of the Polyelectrolyte Molecular Weight on Exponentially Growing Multilayer Films in the Linear Regime. *Langmuir* **2007**, *23*, 1898–1904.
61. Schöll, A.; Schreiber, F. Thin Films of Organic Molecules: Interfaces and Epitaxial Growth. In *Molecular Beam Epitaxy*; Henini, M., Ed.; Elsevier: Oxford, 2013; pp 591−609.
62. Cini, N.; Tulun, T.; Decher, G.; Ball, V. Step-by-Step Assembly of Self-Patterning Polyelectrolyte Films Violating (Almost) All Rules of Layer-by-Layer Deposition. *J. Am. Chem. Soc.* **2010**, *132*, 8264–8265.
63. Ladam, G.; Schaad, P.; Voegel, J. C.; Schaaf, P.; Decher, G.; Cuisinier, F. *In Situ* Determination of the Structural Properties of Initially Deposited Polyelectrolyte Multilayers. *Langmuir* **1999**, *16*, 1249–1255.
64. Virtual Computational Chemistry Laboratory. http://www.vcclab.org, accessed 2005.
65. Lao, L. L.; Venkatraman, S. S.; Peppas, N. A. A Novel Model and Experimental Analysis of Hydrophilic and Hydrophobic Agent Release from Biodegradable Polymers. *J. Biomed. Mater. Res., Part A* **2009**, *90*, 1054–1065.
66. Shukla, A.; Fuller, R. C.; Hammond, P. T. Design of Multidrug Release Coatings Targeting Infection and Inflammation. *J. Controlled Release* **2011**, *155*, 159–166.
67. Li, C.-R.; Yang, X.-Y.; Lou, R.-H.; Zhang, W.-X.; Wang, Y.-M.; Yuan, M.; Li, Y.; Chen, H.-Z.; Hong, B.; Sun, C.-H.; Zhao, L.-X.; *et al. In Vitro* Antibacterial Activity of Vertilmicin and Its Susceptibility to Modifications by the Recombinant AAC(6′)-APH(2″) Enzyme. *Antimicrob. Agents Chemother.* **2008**, *52*, 3875–3882.
68. Andrews, J. M. Determination of Minimum Inhibitory Concentrations. *J. Antimicrob. Chemother.* **2002**, *49*, 1049.
69. Ince, A.; Schutze, N.; Hendrich, C.; Jakob, F.; Eulert, J.; Lohr, J. F. Effect of Polyhexanide and Gentamycin on Human Osteoblasts and Endothelial Cells. *Swiss Med. Wkly.* **2007**, *137*, 139–145.